Quantifying the impact of furnace heat transfer parameter uncertainties on the thermodynamic simulations of a biomass retrofit.

Roeland De Meulenaere[a,b,*], Diederik Coppitters[a,b,c], Tim Maertens[d], Francesco Contino[c], Julien Blondeau[a,b]

[a] *Thermo and Fluid Dynamics (FLOW), Vrije Universiteit Brussel (VUB), Pleinlaan 2, 1050 Brussels, Belgium*
[b] *Brussels Institute for Thermal-fluid systems and clean Energy (BRITE), Vrije Universiteit Brussel (VUB) and Université Libre de Bruxelles (ULB), 1050 Brussels, Belgium*
[c] *Institute of Mechanics, Materials and Civil Engineering (iMMC), Université Catholique de Louvain (UCLouvain), Place du Levant, 2, 1348 Louvain-la-Neuve*
[d] *Onyx Power, Missouriweg 69, 3199 LB Maasvlakte, The Netherlands*

Abstract

High-fidelity thermodynamic simulation software is available to perform detailed simulations of power plants. However, these models depend on many operating parameters the user must characterize to assess the power plant performances. Unfortunately, most parameters are underdetermined by experience: the validation of the model using field measurements does not allow for the complete determination of all parameters, notwithstanding the unavoidable uncertainties of the measurements themselves. These limitations can result in a drastic mismatch between simulated and actual performance and lead to biased, suboptimal decision-making. To address these limitations, we performed Uncertainty Quantification on key furnace heat transfer parameters to predict the thermodynamic performance of coal-fired power plants retrofitted to biomass (co-)firing under uncertain operating conditions. We used a high-fidelity Thermoflex® model to simulate the thermodynamic performance of the power plant, and we adopted Polynomial Chaos Expansion to perform Uncertainty Quantification in a computationally-efficient manner. Finally, we evalu-

*Corresponding author
Email address: roeland.de.meulenaere@vub.be (Roeland De Meulenaere)

ated the effect of various fractions of biomass in the fuel (from 0 to 100%) on the performance, which provides additional information in the decision-making process during the retrofit of the power plant. The results illustrate that the uncertainty on the non-uniform radiant flux factor dominates the uncertainty on the power, efficiency and flue gas temperature, meaning that efforts should aim at reducing the epistemic uncertainty on the radiative heat flux in the boiler. Increasing the biomass fraction results in a decrease in the gross power and gross efficiency. The mean Furnace Exit Gas Temperature remains relatively stable, but reaches a minimum value at 60% biomass co-firing. In conclusion, Polynomial Chaos Expansion allows for a computationally-efficient probabilistic assessment of non-validated operational conditions, such as a fuel switch, in high-fidelity models for thermal power plants. Future work will focus on extending the number of uncertain parameters.

Keywords: Biomass, Uncertainty Quantification, Thermodynamics, Exergy, Retrofit, Furnace Exit Gas Temperature

---

1. Introduction

Currently, 202 coal-fired power plants are still operating in the European Union. These 202 coal-fired power plants represent 461 coal-fired units or 111 GW_e installed power. The average life span of a coal-fired power plant is approximately 40 to 45 years [1]. If Europe wants to reach the self-imposed goals of reducing their CO_2 emissions by at least 55% by 2030 and achieving net zero emissions by 2050, reducing CO_2 emissions from coal-fired power plants are necessary [2, 3]. Among others, electricity production with net zero emissions from coal-fired power plants can be achieved by converting them to biomass firing. In the European H2020 project Arbaheat, retrofitting a large Ultra-SuperCritical (USC) coal-fired power plant into a biomass-fired Combined Heat and Power (CHP) unit with an integrated steam explosion plant and a biorefinery is studied [4, 5]. One of the main challenges is to predict the impact of such a retrofit on the thermodynamic performances of the plant.

A power plant is a complex system, consisting of different mass and energy streams. To address these complex interactions, dedicated software are typically adopted [6–8]. Thermoflex® is an engineering software package of Thermoflow® which enables to perform static thermodynamic (energy and mass balance) simulations of power production facilities [5, 9].

Even if high-fidelity thermodynamic simulation software are available, many operating parameters must be characterized by the user to assess the power plant performances. Unfortunately, the values of all these parameters are underdetermined by experience: the validation of the model using field measurements does not allow for the complete determination of all parameters, notwithstanding the unavoidable uncertainties on the measurements themselves.

Therefore, extrapolating the performances of an existing plant to other operational conditions, including a fuel switch, leads to even more uncertainty on the values of these internal parameters. They include, for instance, detailed characteristics of specific processes, for which no experimental data is available or difficult to acquire, e.g., the flame behaviour in the furnace. For such parameters, values are generally characterized by expert judgement or guessed. This approach can lead to a mismatch between expected and actual performances. To address this issue, these parameters can be characterized by a given uncertainty.

Defining the uncertainty on a model parameter can generally be divided into two categories: epistemic and aleatory uncertainty [10]. Epistemic uncertainty relates to the lack of knowledge on the parameter, which can be improved by increasing the confidence through, e.g., enlarged data collection or using more detailed models. Aleatory uncertainty represents the unknown evolution of the parameter, e.g., the future evolution, and is therefore irreducible [11]. Generally, uncertainty characterization in energy systems does not distinguish between both types of uncertainty. Instead, the parametric uncertainty is represented using probabilistic or non-probabilistic approaches [12]. In a probabilistic approach, the uncertain parameter is characterized by a Probability Density Function (PDF). Such a PDF is typically estimated by statistical inference when a large amount of data is available (e.g., measurement data), by expert judgement when no data is available, or by Bayesian inference when the dataset is limited, but expert knowledge is at hand [13]. Whenever PDFs are assigned to model parameters in energy systems, the distributions are usually assumed to be normally or uniformly distributed [12]. Non-probabilistic approaches include interval analysis, fuzzy set theory and stochastic processes, like Markov chains [14].

To understand the importance of uncertain input parameters on the performance of the system, Uncertainty Quantification (UQ) is typically adopted. The state-of-the-art method that propagates parameter uncertainties through a system model and quantifies the statistical moments of the model output is crude Monte Carlo Simulation (MCS) [15]. Despite always-converging and easy to implement, Monte Carlo Simulation converges slowly, i.e., $10^3 - 10^4$ training samples are typically required [16]. Alternatively, surrogate-assisted UQ promises increased computational efficiency. In this approach, a surrogate model is constructed for the input-output relation of the system model, based on a manageable set of training samples (typically in the order of 10^2 samples). Hence, when computationally intensive model evaluations are considered, surrogate-assisted UQ provides a computationally tractable alternative to, e.g., crude Monte Carlo Simulation [16]. Typical surrogate models include Kriging [17, 18], support vector machines [19], ANalysis Of VAriance (ANOVA) [20] and Polynomial Chaos Expansion (PCE) [16, 21]. Once the surrogate model is constructed, PCE enables to quantify the statistical moments (i.e., mean and standard deviation) and the sensitivity indices (i.e., Sobol' indices) analytically through the PCE coefficients. Coppitters et al. [22] used PCE to quantify the statistical moments on the levelized cost of hydrogen for a directly-coupled photovoltaic-electrolyzer system and indicated that the uncertainty on the discount rate and investment cost of the electrolyzer unit are the main drivers of the uncertainty on the levelized cost of hydrogen. Rixhon et al. [23] used PCE to quantify the Sobol' indices on the cost of the future Belgian energy mix and highlighted the significant importance of the uncertainty related to the cost of electrofuels.

As stated above, performing detailed thermodynamic simulations of power plants depends on a multitude of model parameters. Generally, the values of these parameters are based on assumptions or expert judgement and considered deterministic, i.e., fixed and free from inherent variation. Whenever parametric uncertainties are considered, the simulation models are simplified, to reduce the computational cost of UQ on such a system. However, simplified models carry a significant model-form uncertainty, which reduces the fidelity of the UQ results. Combined, these simplifications can result in a drastic mismatch between simulated and actual performance and consequently lead to biased, suboptimal decision-making process.

To accurately predict the performances of a plant after a biomass retrofit while addressing these limitations, we used an existing, high-fidelity thermodynamic model of a power plant validated for a limited share of biomass and we characterized the uncertainty on two key parameters of the model that generally prove difficult to extrapolate to non-validated conditions: the radiant flux past screen factor and the non-uniform radiant flux factor, both related to the heat transfer process in the furnace. Then we performed UQ in a computationally-efficient manner using PCE. This novel approach allows to accurately define the importance of the uncertainty on these parameters to the performance of the biomass co-fired power plant. We evaluated the effect of various fractions of biomass in the fuel (from 0 to 100%) on the performances, which provides additional information in the decision-making process during the retrofit of the power plant.

The studied power plant and its thermodynamic model are described in Section 2. The studied input parameters, the probabilistic UQ method that was used, and the selected performance indicators are defined in Section 3. The simulations results are discussed in Section 4.

2. Thermodynamic model of a retrofitted plant

In this section, a large-scale power plant of which the retrofit was studied in previous works using a deterministic approach, and the resulting thermodynamic model, are briefly described. The model will be used as a basis for this work.

2.1. The Power Plant

The studied power plant (Figure 1)is a modern 730 MW_e USC coal-fired power plant located in the Netherlands. The power plant was commissioned in 2015 and has a net electrical efficiency of around 45%. The feedwater is preheated by 5 low-pressure preheaters before going into the deaerator. After the deaerator, the feedwater is routed, by several pumps, through 3 high-pressure preheaters to the 1550 MW_{th} USC boiler. The boiler consists of an economiser, 3 superheaters and 2 reheaters (Figure 2). The steam leaving the last superheater has a pressure of 252 bar with a temperature of 600 °C. The reheater will re-increase the temperature to 620 °C while the remaining steam pressure is still 61 bar. The walls of the boiler act as an evaporator[1]. After the boiler, the steam drives one high, one intermediate and two double flow low pressure steam turbines. Afterwards, the used steam arrives in one of the two water cooled condensors.

[1]"Evaporator" is the customary term for the radiative heat exchanger in the furnace, although the cycle is supercritical in this case and, therefore, does not present an evaporation phase as such.

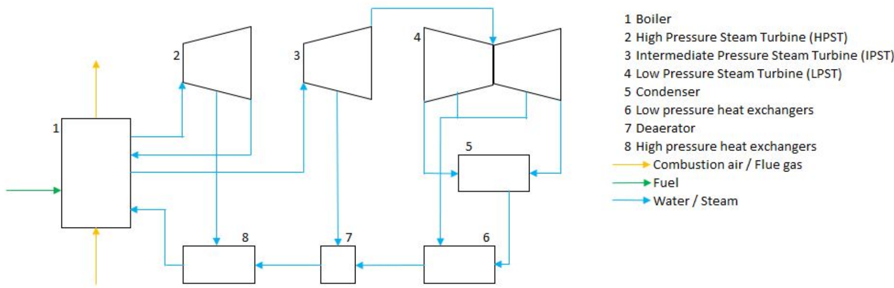

Figure 1: Simplified schematic of the steam cycle. [5]

Several fans direct the combustion air over the rotating air preheater to the boiler. Part of this combustion air will pass through the coal mills to one of the four burners in one of the four burner rows. The flue gas passes a state-of-the-art Flue Gas Treatment (FGT): an ElectroStatic Precipitator (ESP), a Selective Catalytic Reduction (SCR), denitrification system (deNO$_x$) and a wet scrubber desulfurization system (deSO$_x$) forced by an Induced Draught (ID) fan. Finally, the cleaned flue gas will be released in the air through the stack [5].

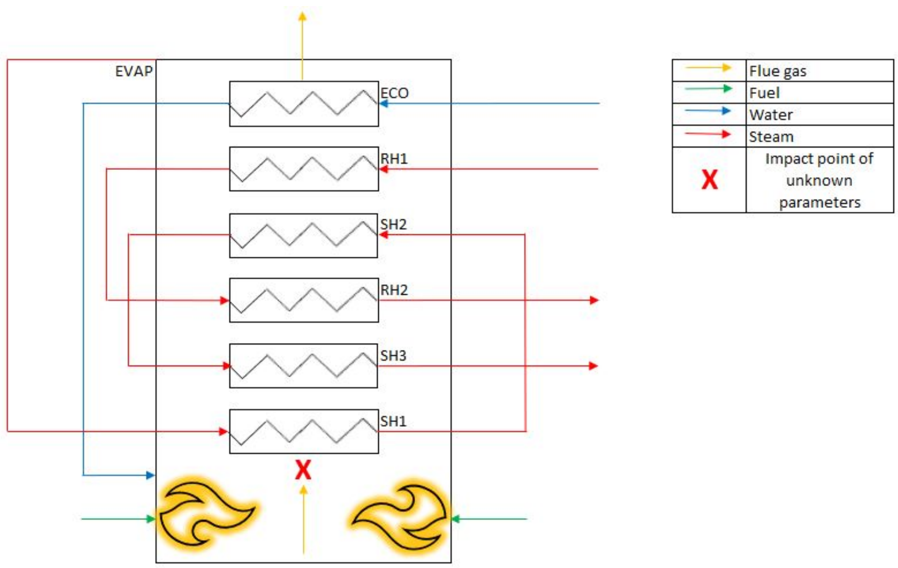

Figure 2: Boiler overview: economizer (ECO), evaporator (EVAP), superheaters (SH) and reheaters (RH).

2.2. Thermodynamic modelling of the biomass retrofit

2.2.1. Base-case model and validation

In previous works, we developed a thermodynamic model of the plant using Thermoflex® [5]. Thermoflex® is a state-of-the-art heat balance software featuring a graphic users interface. It is the most flexible and adaptable package of the Thermoflow® software and is a fully flexible engineering tool to model and to simulate the thermodynamic behaviour of power production facilities (CCGT, CFPP, nuclear, renewables, ...) by calculating the heat and mass balances. With the over two hundred different predefined components models can be made. After composing the model, the default values of the components can be adapt in three stages: thermodynamic mode, engineering mode and the off-design mode. In the thermodynamic mode the model will be calculate on thermodynamic design assumptions. In the next phase (engineering mode) the model will be translate to physical realistic components. Afterwards the model can be frozen in off-design mode and simulations can be performed. This heat balance software calculates first all the pressures in the system, when an equilibrium is reached, all the flows will be calculated followed with all the other parameters. This simulations are static, but with the ELink application, the model can be run quasi dynamic [9]. Based on the original diagrams, specifications and operational data, a base-case model of the plant was developed for full load operation with coal. The base-case model has been validated against the acceptance test results. The acceptance test is the official test performed during the commissioning of the power plant to assess its original efficiency against the design values. As the retrofit to biomass-firing is studied for the current state of the plant, ageing of its components had to be taken into account in the assessment of its performances. Therefore, the model was modified to the current situation and validated against a recent performance test, for 100% coal firing. As stated above, such a conventional validation based on key performance indicators however underdetermines the detailed parameters of the model and requires expert judgment. The model developed and validated in [5] for coal-firing is used as a basis in this paper. While [5] has focused on the energetic and exergetic impact of a retrofit from a coal fired power plant to a biomass CHP with different loads using a deterministic approach, this paper focuses on the impact of unknown parameters on the plant performances, because in the previous paper shortcomings were observed on certain parameters. For the sake of clarity the research for this paper was only done on a fuel switch without a CHP extension.

2.2.2. Biomass co-firing test burns

Furthermore, the conversion of the plant to biomass-firing was studied in the same work [5], through the replacement of coal by steam-exploded Arbacore pellets (Table 1). When compared to traditional wood pellets, steam-exploded pellets are hydrophobic, and the cellulose fibres are broken during the steam explosion process, whereby their structure becomes comparable with the structure of coal. This increases the grindability and the volumetric and energetic density of the biomass pellets, leading to lower requirements in terms of adaptation of the power plant, and thus lower investment costs for a retrofit [24–26]. Nevertheless, these pellets are more expensive, which results in a higher operating cost. These higher operating costs can be partly compensated by extracting the high valuable components (e.g., fulfural) out of the steam-explosion condensate through a bio-refinery [27].

During the summer of 2019, steam-exploded pellet test burns have been performed on the power plant. 22 mass% biomass co-firing was compared to 100% coal-firing. Based on the performed measurements, the thermodynamic model was adapted to be validated against partial biomass co-firing. The modification of some parameters of the model was again carried out using expert judgment, in order to reproduce the observed performances [5].

2.2.3. Predicting plant performances for higher biomass shares

The validated model was then used to predict the performances of the fully converted plant into biomass firing. In this paper, this validated model will be

Table 1: Measured composition of the Arbacore steam exploded pellets and coal.

parameter	unit	pellets value	coal value
Carbon	mass%	53.1	62.43
Hydrogen	mass%	6.05	4.03
Nitrogen	mass%	0.05	1.46
Chlorine	mass%	0.01	0.1
Sulfur	mass%	0.02	1.23
Moisture	mass%	14.5	6.31
Oxygen	mass%	25.84	10.22
LHV	kJ/kg	20,060	24,221

used in a deterministic way to predict the performances of the plant for higher shares of biomass co-firing, up to complete conversion. To properly compare the different co-firing fractions, the heat input in the boiler was kept constant. This resulted in an increasing fuel flow with an increase in the biomass co-firing fraction. However, the global fuel flow remained below the maximum possible fuel flow of 100 kg/s, as described in the specifications of the power plant.

3. Performance assessment using UQ

In this paper, an UQ is used to provide a probabilistic assessment of the performances of the plant for high shares of biomass, with a focus on furnace heat transfer parameters. Radiative heat transfer in the furnace is indeed the process which will be the most impacted by a fuel switch. It is also not modelled in details in thermodynamic models: lump parameters are used to account for uneven heat transfer distribution.

3.1. Radiative heat transfer parameters

Changing the fuel from coal to steam-exploded pellets induces unknown combustion dynamic and kinetic changes in the boiler. Hence, the corresponding radiative and convective heat exchanges become uncertain. In Thermoflex®, in addition to the calculation of the emissivity of the flame based on the flue gas composition, the radiative heat transfer in the furnace is inherently defined by two parameters that are difficult to extrapolate: the *radiant flux past screen factor* and the *non-uniform radiant flux factor*. They are used as correction factors applied to the radiative heat transfer models implemented in Thermoflex to account for the specific composition of various fuels. Unlike many other parameters, their values cannot be assessed based on the results of heat, mass and species balances performed for the boiler. UQ will therefore be applied to them: first to quantify the impact of the related uncertainties, and then to propagate them to assess the resulting uncertainties on the predicted performances. To understand this two parameters better, it is important to know that Thermoflex® calculates the radiative and convective heat exchanges, based on standard coal compositions. Both parameters are correction factor for the deviation of the standard coal compositions [28–30].

3.1.1. Radiant flux past screen

The *Radiant flux past screen* factor defines the fraction of radiation flux directly transferred to the first heat exchanger that is situated downstream of the furnace [9]. The first superheater (or parallel superheaters) is located by Thermoflex® in the gas path following the radiant boiler. This radiation will be considered as heat input to this component. This parameter is critical when considering different fuels, as different fuels cause different heat flux distributions in the furnace. Based on expert judgement, this parameter should range between 80% and 100% [9]. As an equal probability is assumed for each value in between this range, a uniform distribution is considered to characterize the uncertainty on the *Radiant flux past screen factor*. To give better insights on this parameter, a simulation has been performed on the 100% coal model. With *Radiant flux past screen factor* as only variable parameter, 80% resulted in a gross power of 703.4 MW and a gross efficiency of 46.60% and 100% resulted in decreased gross power and gross efficiency of 702.6 MW and 46.55%, respectively.

3.1.2. Non-uniform radiant flux factor

The *Non-uniform radiant flux factor* parameter corresponds to a heat transfer non-uniformity correction factor, which accounts for the non-uniform distribution of the heat flux within the furnace [9]. Typically, these heat fluxes are highest in the lower furnace region. When flowing upwards towards the furnace exit, these fluxes diminish [9]. As changing the fuel will impact the combustion dynamics, combustion kinetics and burn out of the fuel particles in the boiler, the radiation of the burning gases and particles will vary. Based on expert judgement, this parameter should range between 70% and 100%. As an equal probability is assumed for each value in between this range, a uniform distribution is considered to characterize the uncertainty on the *Non-uniform radiant flux factor*. For *Non-uniform radiant flux factor* the same simulation as for *Radiant flux past screen factor* has been executed, but with *Non-uniform radiant flux factor* as only variable parameter. For the gross power this resulted in an increase from 702.2 MW to 703.5 MW and for the gross efficiency from 46.52% to 46.60%.

3.2. Polynomial Chaos Expansion

We adopted Polynomial Chaos Expansion (PCE), a probabilistic UQ approach, to propagate the probabilistic input parameter uncertainties through the system model, quantify the statistical moments on the quantities of interest, and determine the Sobol' indices [11]. To apply PCE on the thermal power plant model, we used the open-source Python framework RHEIA [31], developed in our research group. A PCE model ($\hat{M}$) replicates the function that represents the relation between the input parameters and the output parameter of interest defined in the Thermoflex model (M). This PCE representation consists of a truncated series of multivariate orthonormal polynomials $\boldsymbol{\Psi}$, weighted by coefficients u:

$$\hat{M}\left(\boldsymbol{\xi}\right) = \sum_{\boldsymbol{\alpha} \in \mathcal{A}^{d,p}} u_{\boldsymbol{\alpha}} \boldsymbol{\Psi}_{\boldsymbol{\alpha}}\left(\boldsymbol{\xi}\right) \approx M\left(\boldsymbol{\xi}\right), \tag{1}$$

where $\boldsymbol{\xi} = (\xi_1, \xi_2)$ represents the vector of the independent random parameters, d corresponds to the number of input distributions and $\boldsymbol{\alpha}$ is a multi-index. The truncation scheme limits the number of multivariate polynomials in the series based on a limiting polynomial order p and the number of uncertain parameters ($d = 2$). The multivariate polynomial order $|\boldsymbol{\alpha}|$ is the sum of the order for each univariate polynomial in the multivariate polynomial. Therefore, the multi-indices that correspond to an order below or equal to the limiting order p are stored in the truncated series $\mathcal{A}^{d,p}$:

$$\mathcal{A}^{d,p} = \left\{\boldsymbol{\alpha} \in \mathbb{N}^d : |\boldsymbol{\alpha}| \leq p\right\}. \tag{2}$$

The amount of existing multi-indices that comply with this rule equals:

$$\operatorname{card}\left(\mathcal{A}^{d,p}\right) = \binom{p+d}{p} = \frac{(d+p)!}{d!p!} = P + 1. \tag{3}$$

In conclusion, the PCE representation for this model reads:

$$\hat{M}\left(\xi_1, \xi_2\right) = \sum_{\boldsymbol{\alpha} \in \mathcal{A}^{d,p}} u_{\boldsymbol{\alpha}} \boldsymbol{\Psi}_{\boldsymbol{\alpha}}\left(\xi_1, \xi_2\right). \tag{4}$$

As uniform distributions are considered, the Legendre polynomials are adopted, as they are the associated family of polynomials that are orthogonal with respect to standard uniform distributions [16]. For a maximum polynomial degree of 3, the truncation set $\mathcal{A}^{2,3}$ contains 10 multi-indices (Equation 3). The 10 corresponding multivariate polynomials and the normalized Legendre polynomials up to order 3 are presented in Table 2.

Hence, the PCE model $\hat{M}\left(\xi_1, \xi_2\right)$ for the Thermoflex model $\mathcal{M}\left(\xi_1, \xi_2\right)$ is the sum of all multivariate polynomials, weighted by the coefficients (after reducing ξ_1 and ξ_2 to standard uniform distributions):

$$\begin{aligned}\hat{M}\left(\xi_1, \xi_2\right) = u_0 + \frac{\sqrt{3}}{3}\,\xi_1 u_1 + \frac{\sqrt{3}}{3}\,\xi_2 u_2 + u_3 \frac{\sqrt{5}}{5}\,\frac{3\xi_1^2 - 1}{2} + u_4 \frac{\xi_1 \xi_2}{3} + \\ u_5 \frac{\sqrt{5}}{5}\,\frac{3\xi_2^2 - 1}{2} + u_6 \frac{\sqrt{7}}{7}\,\frac{5\xi_1^3 - 3\xi_1}{2} + u_7 \xi_2 \frac{3\xi_1^2 - 1}{2\sqrt{15}} + \\ u_8 \xi_1 \frac{3\xi_2^2 - 1}{2\sqrt{15}} + u_9 \frac{\sqrt{7}}{7}\,\frac{5\xi_2^3 - 3\xi_2}{2}.\end{aligned} \tag{5}$$

To quantify the coefficients $(u_0, \ldots, u_9)$, training samples $\left(\boldsymbol{x}^{(i)} = \left(\xi_{1,i}, \xi_{2,i}\right), i = 1, \ldots, n\right)$ are required. The regression method is adopted to quantify the coefficients for the orthonormal polynomials [16]. To acquire a well-posed least-square

Table 2: The multivariate polynomials.

Ψ	$\boldsymbol{\alpha}$	$\boldsymbol{\Psi}_{\boldsymbol{\alpha}}$
$\Psi_0\left(x\right)=1$	$(0,0)$	1
$\Psi_1\left(x\right)=\frac{\sqrt{3}}{3}\;x$	$(1,0)$	$\frac{\sqrt{3}}{3}\;\xi_1$
$\Psi_2\left(x\right)=\frac{\sqrt{5}}{5}\;\frac{3x^2-1}{2}$	$(0,1)$	$\frac{\sqrt{3}}{3}\;\xi_2$
$\Psi_3\left(x\right)=\frac{\sqrt{7}}{7}\;\frac{5x^3-3x}{2}$	$(2,0)$	$\frac{\sqrt{5}}{5}\;\frac{3\xi_1^2-1}{2}$
	$(1,1)$	$\frac{\xi_1\xi_2}{3}$
	$(0,2)$	$\frac{\sqrt{5}}{5}\;\frac{3\xi_2^2-1}{2}$
	$(3,0)$	$\frac{\sqrt{7}}{7}\;\frac{5\xi_1^3-3\xi_1}{2}$
	$(2,1)$	$\xi_2\frac{3\xi_1^2-1}{2\sqrt{15}}$
	$(1,2)$	$\xi_1\frac{3\xi_2^2-1}{2\sqrt{15}}$
	$(0,3)$	$\frac{\sqrt{7}}{7}\;\frac{5\xi_2^3-3\xi_2}{2}$

minimization, the empirical rule of thumb is to have a number of training samples equal to at least two times the number of coefficients [16]. Hence, $2\left(P+1\right)$ samples are evaluated in the system model, and the model response for each quantity of interest is stored. The quasi-random Sobol' sampling technique is adopted to generate the training samples [32]. While the basis function for the PCE (Eq. 5) is the same, the coefficients are different for each case (i.e., different fractions of biomass) and for each output (i.e., gross power, gross efficiency and the Furnace Exit Gas Temperature (FEGT)).

To estimate the error of the PCE, Leave-One-Out (LOO) cross-validation is considered. First, a PCE is constructed without the information from one training sample $\boldsymbol{x}^{(i)}$, i.e., $\hat{M}^{\setminus i}$. After that, the residual error is quantified on the sample that has been left out as the difference between the result from the actual model M and the result from the PCE without information on that point $\hat{M}^{\setminus i}$:

$$\Delta_i = M\left(\boldsymbol{x}^{(i)}\right) - \hat{M}^{\setminus i}\left(\boldsymbol{x}^{(i)}\right). \tag{6}$$

This process is repeated for each sample. With $2\,(P+1)$ training samples, the LOO error is the sum of the $2\,(P+1)$ residual errors:

$$E_{\mathrm{LOO}} = \frac{1}{2\,(P+1)} \sum_{i=1}^{2(P+1)} \Delta_i^2. \tag{7}$$

However, this approach can be cumbersome as it requires constructing $2\,(P+1)$ PCEs. However, the same result can be acquired from a single PCE, using the diagonal terms h_i in the least-square minimization matrix. We refer to Sudret [16] for additional details on the algebraic derivations. Finally, the LOO error is quantified as:

$$E_{\mathrm{LOO}} = \frac{1}{2\,(P+1)} \sum_{i=1}^{2(P+1)} \left(\frac{M\left(\boldsymbol{x}^{(i)}\right) - \hat{M}\left(\boldsymbol{x}^{(i)}\right)}{1-h_i}\right). \tag{8}$$

Note that in this formulation, $\hat{M}$ is constructed based on the full experimental design (i.e., 20 training samples). The LOO error is normalized by the variance of the model outputs.

Using the LOO error, the maximum polynomial degree for the polynomials p was determined such that the PCE is accurate. To define the polynomial degree, the polynomial degree is increased incrementally until a sufficient accuracy is achieved [31]. Starting from $p = 1$, a PCE is constructed. If the LOO error is below a certain threshold, the corresponding polynomial order is considered sufficient to generate an accurate PCE. If not, the order is increased and additional samples are generated based on Eq. 3. In this work, a polynomial order of 3 is required (20 training samples, Eq. 3) to result in a LOO error below 1 % for each output considered (i.e., gross power, gross efficiency and the FEGT).

Finally, the statistical moments can be derived from the PCE coefficients analytically, i.e., no more model evaluations are required. To illustrate, the mean μ and standard deviation σ are derived as follows:

$$\mu = u_0, \tag{9}$$

$$\sigma^2 = \sum_{i \neq 0} u_i^2. \tag{10}$$

In addition, the Sobol' indices can be quantified analytically as well. The total-order Sobol' indices (S_i^T) quantify the total impact of a stochastic input parameter on the performance indicator, including all interactions:

$$S_i^T = \sum_{\boldsymbol{\alpha} \in A_i^T} u_{\boldsymbol{\alpha}}^2 / \sum_{i=1}^{P} u_i^2 \qquad A_i^T = \{\boldsymbol{\alpha} \in A | \alpha_i > 0\}, \tag{11}$$

where A is the set of all the PCE coefficients and α_i represents the coefficient related to uncertain parameter i.

3.3. Energetic and Exergetic analysis

To evaluate the power plant performance for different fuel compositions, an energetic and exergetic boiler analysis is adopted. In the next two paragraphs, quantities of interest for both analyses are defined.

3.3.1. Energetic boiler efficiency

The energetic boiler efficiency η_{boiler} of the power plant is defined as follows:

$$\eta_{boiler} = \frac{P_{\text{exchanged}}}{P_{\text{fuel}}} \text{ [-]}, \tag{12}$$

where $P_{\text{exchanged}}$ corresponds to the increase in energy of the water and the steam over the heat exchangers in the boiler. Hence, the energy exchange between the flue gas and the water/steam cycle multiplied with water/steam flow through the heat exchangers. P_{fuel} is the thermal power input for the boiler, calculated as the product of the fuel flow rate and its Lower Heating Value (LHV).

3.3.2. Exergetic boiler efficiency

The exergetic boiler efficiency, $\eta_{\psi,boiler}$, is defined as:

$$\eta_{\psi,boiler} = \frac{P_{\psi,\text{exchanged}}}{P_{\psi,\text{fuel}}} \text{ [-]}, \tag{13}$$

where $P_{\psi,\text{exchanged}}$ is the exchanged exergy between the flue gas and the water/steam cycle and $P_{\psi,\text{fuel}}$ is the exergy input of the fuel, calculated as the product of the fuel flow rate and its exergy content ψ_{fuel}.

The exchanged exergy between the flue gas and the water/steam cycle is defined as the sum of the products of the water/steam flow through the heat exchangers with the exergy, ψ_{heat}, difference of the water/steam over the heat exchangers:

$$\psi_{\text{heat}} = (h - h_0) - T_0(s - s_0) \text{ [kJ/kg]}, \tag{14}$$

where T_0, the absolute temperature is 19.4 °C (cooling water temperature), h the enthalpy and s the entropy. The subscript 0 refers to environment.

The exergy content ψ_{fuel} is calculated using the correlations proposed by Kostas [33], to calculate the ratio ϕ between the exergy content of a fuel and its LHV:

$$\phi = \frac{\psi_{fuel}}{LHV} \text{ [-]}. \tag{15}$$

For a dry solid fuel with an O/C ratio lower than 0.667, Kostas [33] proposed the following correlation:

$$\phi_{\text{dry}} = 1.0437 + 0.1882\ \frac{m_{\text{H}_2}}{m_{\text{C}}} + 0.061\ \frac{m_{\text{O}_2}}{m_{\text{C}}} + 0.0404\ \frac{m_{\text{N}_2}}{m_{\text{C}}} \text{ [-]}\ , \tag{16}$$

where m_X is the mass concentration of element X in the fuel. The following correction is proposed to account for the moisture and sulfur contents of the fuel when calculating its exergy content [33]:

$$\psi_{fuel} = \big((LHV + 2442\ w)\ \phi_{dry} + 9417\ m_S\big) \text{ [kJ/kg]}, \tag{17}$$

where w is the mass fraction of the moisture in the fuel (as received).

4. Results and Discussion

In order to assess the impact of the uncertain parameters on the power plant performance for a reference case, the UQ method is first applied to the case of the test burn performed in 2019, i.e. for a 22% share of biomass (Subsection 4.1). Thereafter, the impact of these uncertainties on the gross power, gross efficiency and the Furnace Exit Gas Temperature (FEGT) is assessed for increasing shares of biomass, up to full conversion (Subsection 4.2).

4.1. 22% biomass co-firing

20 training samples are generated on the two uncertain parameters using a quasi-random Sobol' sampling and evaluated in the high-fidelity Thermoflex® model (the other parameters are considered fixed, based on the measurements during the test burn). The deterministic response of these simulations are used to construct the PCE surrogate model. From this PCE, the statistical moments on the gross power and efficiency are calculated. A mean gross power of 702.0 MW with a standard deviation of 0.5 MW is retrieved (Figure 3). Following the parametric uncertainty considered, the actual performance situates within 700.8 MW and 702.9 MW over a range of 3σ or a deviation of 0.39%. However, due to the shape of the probability density functions, a performance near 702.0 MW achieves the highest probability. The measured gross power during the test burn (701.9 MW) situates within the uncertainty range on the calculated gross power. The mean efficiency is 46.50 % with a standard deviation of 0.03 % (Figure 3). The actual efficiency situates between 46.42 % and 46.57 % over a range of 3σ. Based on the shape of the probability density functions, an efficiency of 46.52 % has the highest probability.

It can be observed that the distribution on the power is skewed after the propagation of the uniform distributions through the model (Figure 3, top). This follows from the non-linear interactions in the model, mainly related to radiative heat transfer in this case. To clarify the distribution shape, 10^4 samples were evaluated and their resulting power and efficiency is plotted with respect to the non-uniform radiant flux factor (Figure 3, middle) and the radiant flux past screen (Figure 3, bottom). The height of the plane at each power output (resp., efficiency) illustrates the probability of realizing this value for the corresponding input parameter. Hence, the peak of the distribution is located on the power (resp., efficiency) axis where the sum of the two heights is the highest.

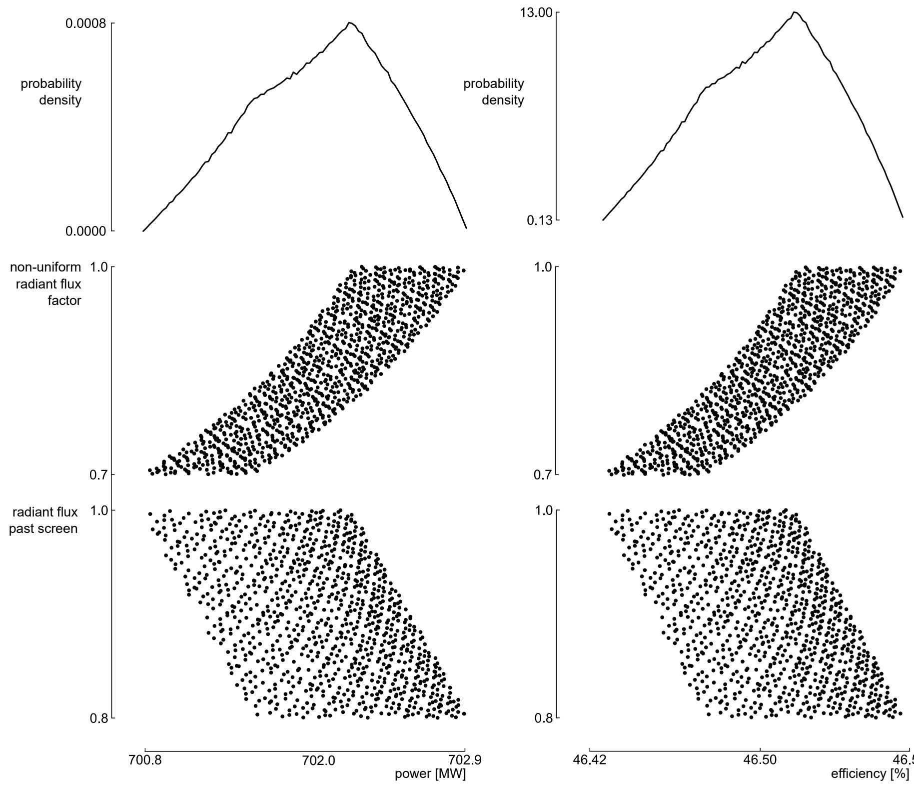

Figure 3: The distributions of the gross power and gross efficiency for 22% biomass co-firing.

4.2. 0% to 100% biomass co-firing

In this section, the predicted gross power, gross efficiency and Furnace Exit Gas Temperature (FEGT) are assessed in a probabilistic way up to full conversion to biomass. A series of probability distribution functions are therefore generated for each of these parameters, showing their evolution when moving towards full conversion.

4.2.1. Gross power and gross efficiency

Figure 4 shows the evolution of the probability densities of the gross power and the gross efficiency of the plant for an increasing share of biomass.

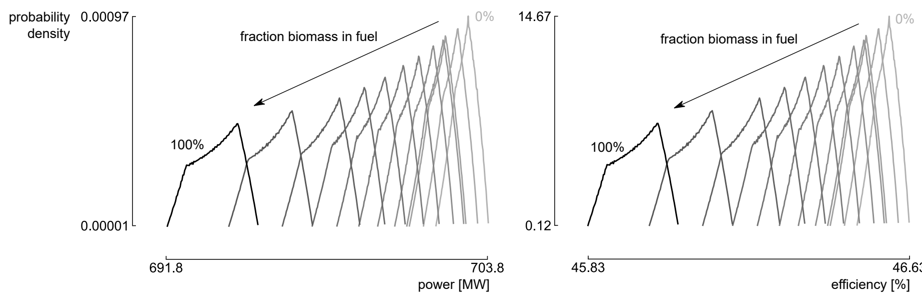

Figure 4: The distributions of the gross power (left) and gross efficiency (right) for different biomass fractions in the fuel.

These results show that the mean gross produced power will decrease from 703.0 MW for no biomass co-firing to 693.7 MW for the full re-conversion to biomass. The standard deviation will increase with an increasing biomass fraction from 0.4 MW (only coal) to 0.8 MW (only biomass). The mean gross efficiency of the power plant will decrease from 46.57% (only coal) to 45.95% (only biomass). The related standard deviation is also increasing with an increasing biomass fraction, from 0.03% to 0.05%. The gross power and the efficiency are therefore both subject to an increasing uncertainty for an increasing biomass fraction (Figure 5, middle).

This increase in the uncertainty is analysed through the evolution of the Sobol' indices (Figure 5, bottom). They give the contribution of each parameter to the standard deviation. In other words, they show by how much the standard deviation would be reduced if the parameter was perfectly known. In this case, the uncertainty on the produced power and the efficiency is mainly due to the uncertainty on the *non-uniform flux* parameter. This contribution increases with an increasing biomass share in the fuel.

This behaviour can be explained by invoking the change in the operating parameters of the power plant when switching to biomass. Although the fuel energy input stays the same for all the simulations, the different characteristics

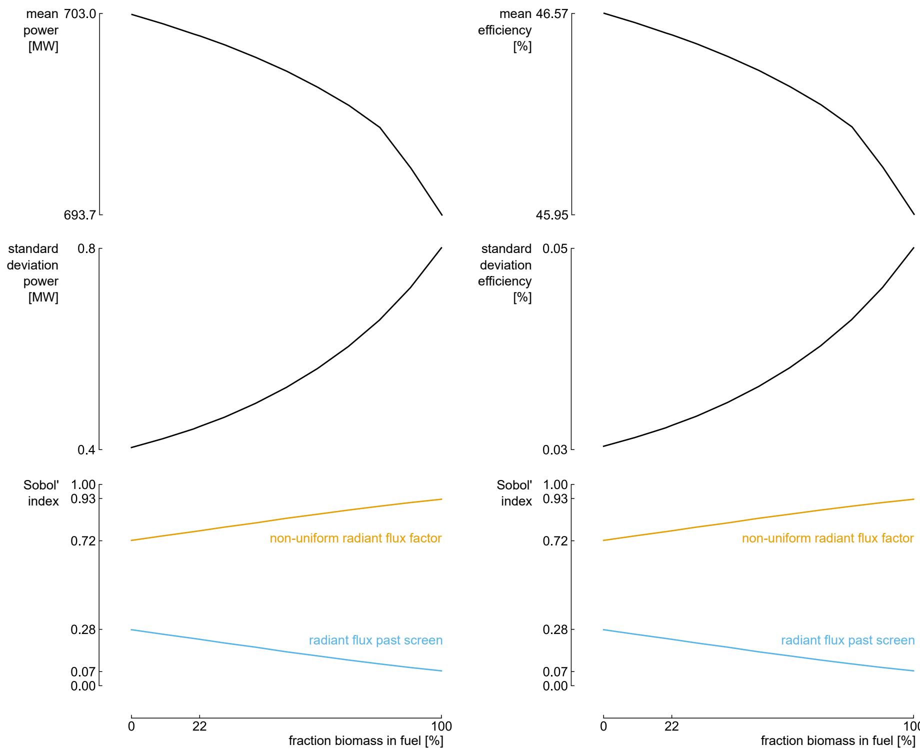

Figure 5: The mean power and the mean efficiency both decrease when increasing the biomass share in the fuel. The related standard deviations increase, meaning that the expected power becomes more uncertain. The Sobol' indices show that the uncertainty on the produced power and the efficiency is mainly due to the uncertainty on the *non-uniform flux* parameter.

of biomass compared to coal lead to a decrease of the produced gross power (Figure 4). First, the LHV of the fuel mix decreases with an increasing biomass fraction because the LHV of coal (24,221 kJ/kg) is higher than the LHV of biomass (20,060 kJ/kg). Second, the moisture content of the biomass (14.5%) is higher than for coal (6.31%). Combined, the combustion of biomass generates more flue gas than coal for a constant boiler heat input. This results in a lower adiabatic flame temperature (Table 3) and therefore in a less radiant heat transfer. To keep the energy input constant, the fuel flow will raise with an increasing biomass fraction. As a consequence, reaching the nominal steam temperature cannot be achieved without decreasing the nominal steam pressure and steam flow rate (Table 3). This corresponds to a loss of both quantity and exergy content of the produced steam. As a consequence, the exergy efficiency of the boiler itself decreases by more than 3% for full conversion, while its energy efficiency decreases by less than 1%, see Figure 6. This loss of quality of the energy delivered to the water/steam flow is the main reason for the decrease of the gross power and the gross efficiency.

Table 3: Differences between pellets and coal for the main resulting parameters in the studied case.

parameter	unit	pellets value	coal value
Steam Temperature	°C	603.1	603.1
Steam pressure	bara	228.9	238.4
Steam flow	kg/s	514.6	539.6
Adiabatic flame temperature	°C	1853.7	2001.8

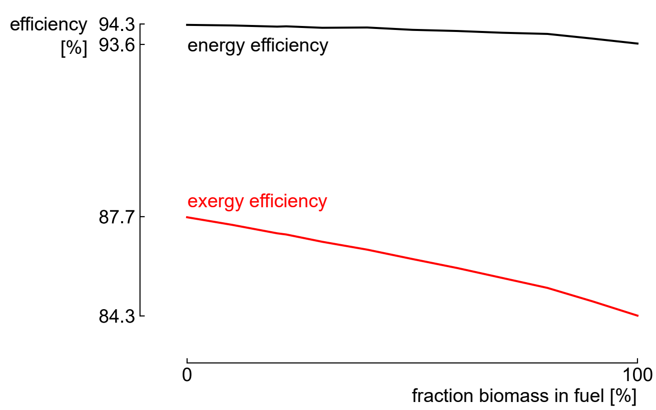

Figure 6: Evolution of the energy and exergy efficiency of the boiler with an increasing biomass co-firing fraction.

Based on the Thermoflex model, the increasing standard deviation with an increasing biomass co-firing fraction is a consequence of several reasons: compared with burning coal, burning biomass will require a higher airflow rate, and will result in a lower flue gas temperature. The biomass flow will be also higher to reach the same energy input. As a consequence, the adiabatic flame temperature in the boiler, will be 2002 °C for 100% coal-firing and 1854 °C for 100% biomass-firing.

4.2.2. Furnace Exit Gas Temperature

An important parameter for coal and biomass-fired power plants is the Furnace Exit Gas Temperature (FEGT). The FEGT is a key performance parameter of the combustion process in boilers, but very difficult to measure [34]. From a thermodynamic point of view, a high FEGT results from a limited heat transfer in the furnace and leads to a higher heat transfer in the convective passes. However, the FEGT can also have several operational implications, e.g., the fact that the FEGT cannot be too high to avoid the deposition of molted ash particles on the convective heat exchangers (slagging). Therefore, any solid fuel must be tested to measure its Ash Fusion Temperature (AFT) [35], which needs to be compared to the FEGT. The norms to determine the AFT in reducing and oxidizing atmosphere are ASTM D1857 and DIN 51730. The AFT of biomass is generally lower than for coal. In general, high fusion temperatures result in low slagging potential in dry bottom furnaces, while low fusion temperatures are considered mandatory for wet-bottom furnaces [36].

Given the importance of this operational parameter, the UQ method is particularly interesting to apply to assess its value. Figure 7 shows the evolution of the probability distribution of the FEGT for increasing shares of biomass.

The distribution of FEGT spreads over 20 to 40 °C, and the spread tends to increase with higher shares of biomass, which would potentially decrease the risk of slagging. The average value is however rather stable, between 1239 °C and 1247 °C. A minimum value can be observed for a biomass co-firing of 60%. It can be explained by two counteracting effects of biomass combustion in the furnace. On the one hand, as explained above, the larger amount of flue gas decreases the radiative heat transfer. But on the other hand, it also increases the convective heat transfer in the furnace. It can therefore be concluded that a lower risk of slagging is expected for 60% biomass co-firing fraction. This, in turn, will decrease the need for soot blowing, leading to a decrease of auxiliary

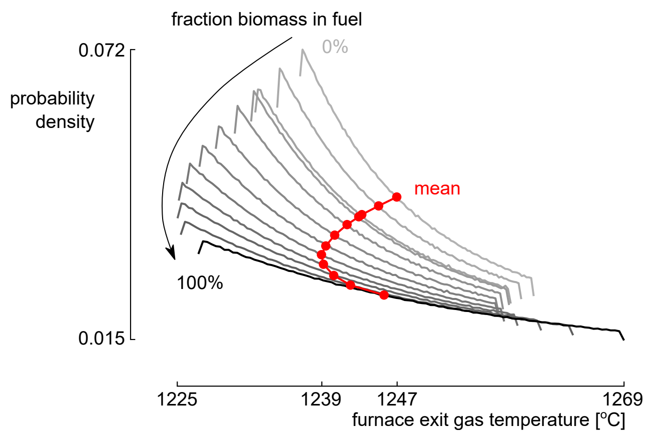

Figure 7: The probability distribution of the Furnace Exit Gas Temperature as a function of the share of biomass.

power losses.

The standard deviation follows the same trend as for the gross power and gross efficiency and increases with a increasing biomass fraction (Figure 7). The standard deviation increases or the accuracy decreases with a increasing biomass fraction from 6.7 °C to 12.2 °C.

5. Conclusions

In this work, UQ has been applied to a high-fidelity Thermoflex® model of a power plant to investigate the effect of uncertainty in the boiler radiative heat transfer parameters when converting a power plant from coal to biomass.

A significant gain in computational efficiency has been achieved by adopting PCE instead of Monte Carlo Simulation, as only 20 training samples are required, instead of 10^{3-5} samples, to calculate the statistical moments and to perform a global sensitivity analysis on the quantities of interest of the power plant. Hence, this methods allows to perform UQ on a high-fidelity Thermoflex® model in a computationally tractable manner.

The uncertainty on the gross power and gross efficiency induced by the uncertainty on the non-uniform radiant flux factor and the radiant flux past screen factor is relatively small. This means that estimating the value for these two parameters within the ranges used in this study will not induce a significant discrepancy between simulated and actual performances.

The uncertainty on the non-uniform radiant flux factor dominates the uncertainty on the power, efficiency and flue gas temperature (Sobol' indices of at least 0.75). This contribution increases with the fraction of biomass in the fuel. Efforts aiming at reducing the epistemic uncertainty on the radiative heat flux in the boiler should therefore focus on this parameter.

Increasing the biomass fraction results in a decrease of the gross power and the gross efficiency. It directly results from a lower exergy efficiency of the boiler, where the nominal temperature cannot be reached without decreasing the steam pressure and the steam flow rate. The related standard deviations increase, but the uncertainty remains tolerable, even for 100% biomass firing.

The mean Furnace Exit Gas Temperature remains relatively constant, but reaches a minimum value for 60% biomass co-firing. The related standard deviation also increases for higher share of biomass.

UQ proved to be an efficient method to carry out detailed thermodynamic simulations of thermal power plants aiming at assessing their performances in a probabilistic way for non-validated operational conditions, such as a fuel switch.

In future work, the stochastic dimension will be extended, to improve the representation of the random operating environment of the power plant for different fuel blends.

6. Acknowledgments

The results of the work presented in this paper were generated within the EU-H2020 project "Cost-effective transformation of a highly-efficient advanced thermal ultra-supercritical coal-fired power plant into a CHP by retrofitting and integrating an ARBAFLAME biomass upgrading process", with the acronym ARBAHEAT. This project has received funding from the European Union's Horizon 2020 research and innovation program under grant agreement No. 818349. The second author acknowledges the support from the Belgian federal Energy Transition Fund, project DRIVER.

References

[1] P. Markewitz, M. Robinius, D. Stolten, The future of fossil fired power plants in germany—a lifetime analysis, Energies 11 (6) (2018). doi:10.3390/en11061616.
URL https://www.mdpi.com/1996-1073/11/6/1616

[2] United Nations, Paris Agreement (2015).

[3] European Commission, The European Green Deal (2019).

[4] Arbaheat, Arbaheat (accessed in Februari 2022).
URL www.arbaheat.eu

[5] R. De Meulenaere, T. Maertens, A. Sikkema, R. Brusletto, T. Barth, J. Blondeau, Energetic and Exergetic Performances of a Retrofitted, Large-Scale, Biomass-Fired CHP Coupled to a Steam-Explosion Biomass Upgrading Plant, a Biorefinery Process and a High-Temperature Heat Network, Energies 14 (22) (2021) 7720.

[6] F. Alobaid, N. Mertens, R. Starkloff, T. Lanz, C. Heinze, B. Epple, Progress in dynamic simulation of thermal power plants, Progress in Energy and Combustion Science 59 (2017) 79–162.

[7] O. J. Khaleel, T. K. Ibrahim, F. B. Ismail, A. T. Al-Sammarraie, Developing an analytical model to predict the energy and exergy based performances of a coal-fired thermal power plant, Case Studies in Thermal Engineering 28 (2021) 101519.

[8] J. Garcet, R. De Meulenaere, J. Blondeau, Enabling flexible CHP operation for grid support by exploiting the DHN thermal inertia, Applied Energy 316 (2022) 119056.

[9] THERMOFLEX®, Version 29, Thermoflow Inc. (USA).
URL www.thermoflow.com

[10] H. Yu, Reliability-based design optimization of structures: methodologies and applications to vibration control, Ph.D. thesis, Ecully, Ecole centrale de Lyon (2011).

[11] D. Coppitters, W. De Paepe, F. Contino, Robust design optimization of a photovoltaic-battery-heat pump system with thermal storage under aleatory and epistemic uncertainty, Energy (2021) 120692.

[12] G. Mavromatidis, K. Orehounig, J. Carmeliet, A review of uncertainty characterisation approaches for the optimal design of distributed energy systems, Renewable and Sustainable Energy Reviews 88 (2018) 258–277.

[13] R. Nadimi, K. Tokimatsu, Analyzing of renewable and non-renewable energy consumption via Bayesian inference, Energy Procedia 142 (2017) 2773–2778.

[14] Z. Kang, Robust design optimization of structures under uncertainties (2005).

[15] R. Y. Rubinstein, D. P. Kroese, Simulation and the Monte Carlo method, Vol. 10, John Wiley & Sons, 2016.

[16] B. Sudret, Polynomial chaos expansions and stochastic finite-element methods, Risk and Reliability in Geotechnical Engineering Chap. 6 (2003) (2014) 265–300.

[17] I. Kaymaz, Application of kriging method to structural reliability problems, Structural Safety 27 (2) (2005) 133–151.

[18] Z. Deng, X. Hu, X. Lin, Y. Che, L. Xu, W. Guo, Data-driven state of charge estimation for lithium-ion battery packs based on Gaussian process regression, Energy 205 (2020) 118000.

[19] B. Richard, C. Cremona, L. Adelaide, A response surface method based on support vector machines trained with an adaptive experimental design, Structural Safety 39 (2012) 14–21.

[20] H. Rabitz, Ö. F. Aliş, General foundations of high-dimensional model representations, Journal of Mathematical Chemistry 25 (2) (1999) 197–233.

[21] D. Coppitters, W. De Paepe, F. Contino, Robust design optimization and stochastic performance analysis of a grid-connected photovoltaic system with battery storage and hydrogen storage, Energy 213 (2020) 118798.

[22] D. Coppitters, W. De Paepe, F. Contino, Surrogate-assisted robust design optimization and global sensitivity analysis of a directly coupled photovoltaic-electrolyzer system under techno-economic uncertainty, Applied Energy 248 (2019) 310–320.

[23] X. Rixhon, G. Limpens, D. Coppitters, H. Jeanmart, F. Contino, The Role of Electrofuels under Uncertainties for the Belgian Energy Transition, Energies 14 (13) (2021) 4027.

[24] C. Løhre, J. Underhaug, R. Brusletto, T. Barth, A workup protocol combined with direct application of quantitative nuclear magnetic resonance spectroscopy of aqueous samples from large-scale steam explosion of biomass, ACS omega 6 (10) (2021) 6714–6721.

[25] D. R. Fosnacht, D. W. Hendrickson, Use of biomass fuels in global power generation with a focus on biomass pre-treatment, Natural Resources Research Institute, University of Minnesota, Duluth (2016) 1–3.

[26] P. S. Lam, Steam explosion of biomass to produce durable wood pellets, Ph.D. thesis, University of British Columbia Vancouver, Canada (2011).

[27] P. Abelha, M. K. Cieplik, Evaluation of steam-exploded wood pellets storage and handling safety in a coal-designed power plant, Energy & Fuels 35 (3) (2021) 2357–2367.

[28] J. M. Beér, J. Clauss, J. Inst. of Fuel 44 (1962) 437.

[29] H. C. Hottel, A. F. Sarofim, Radiative Transfer, McGraw-Hill Book Co., 1967.

[30] A. F. Sarofim, H. C. Hottel, Radiative transfer in combustion chambers: Influence of alternate fuels, in: Proceedings of the 6th Intl. Heat Transfer Conference, Toronto, Canada, 1978.

[31] D. Coppitters, P. Tsirikoglou, W. De Paepe, K. Kyprianidis, A. Kalfas, F. Contino, RHEIA: Robust design optimization of renewable Hydrogen and dErIved energy cArrier systems, Journal of Open Source Software 7 (75) (2022) 4370.

[32] D. Coppitters, K. Verleysen, W. De Paepe, F. Contino, How can renewable hydrogen compete with diesel in public transport? Robust design optimization of a hydrogen refueling station under techno-economic and environmental uncertainty, Applied Energy 312 (2022) 118694.

[33] T. J. Kotas, The exergy method of thermal plant analysis, Krieger Publishing Company, 1995.

[34] J. Blondeau, J. Van den Auweele, S. Alimuddin, F. Binder, F. Turoni, Online adjustment of furnace exit gas temperature field using advanced infrared pyrometry: Case study of a 1500 mwth utility boiler, Case Studies in Thermal Engineering 21 (2020) 100649.

[35] M. Ozer, O. M. Basha, G. Stiegel, B. Morsi, 7 - effect of coal nature on the gasification process, in: T. Wang, G. Stiegel (Eds.), Integrated Gasification Combined Cycle (IGCC) Technologies, Woodhead Publishing, 2017, pp. 257–304.

[36] B. G. Miller, 4 - introduction to coal utilization technologies, in: B. G. Miller (Ed.), Clean Coal Engineering Technology (Second Edition), second edition Edition, Butterworth-Heinemann, 2017, pp. 147–229.